A. Carpinteri et alii, Frattura ed Integrità Strutturale, 41 (2017) 175-182; DOI: 10.3221/IGF-ESIS.41.24

Focused on Crack Tip Fields

Fracture toughness of rough and frictional cracks emanating from a re-entrant corner

Andrea Carpinteri, Andrea Spagnoli, Michele Terzano, Sabrina Vantadori

Department of Engineering and Architecture, University of Parma, Viale Usberti 181/A, 43124 Parma, Italy

spagnoli@unipr.it

ABSTRACT. In mixed-mode conditions, the competing contribution of the different stress intensity factors predicts fracture initiation load as well as crack propagation direction. Commonly, mixed-mode fracture resistance is based on the assumption of smooth and frictionless cracks. However, the effect of friction and roughness cannot be neglected when mixed mode loading occurs, as in the case of a crack emanating from a re-entrant corner. In this paper, the effect of friction and roughness is evaluated through a simple saw-tooth model in a three-quarter-infinite plane (corresponding to a 90 degree re-entrant corner). The crack surfaces are assumed to be globally smooth, and roughness and friction are incorporated through a constitutive law between opposite crack surfaces. The solution is found using the distributed dislocation method, and an iterative algorithm is needed due to the non-linearity of the model. The effect of friction and roughness angle is discussed for a simple case.

KEYWORDS. Fracture toughness; Friction; Roughness; Distributed dislocation method; Re-entrant corner.

Citation: Carpinteri, A., Spagnoli, A., Terzano, M., Vantadori, S., Fracture toughness of rough and frictional cracks emanating from a re-entrant corner, Frattura ed Integrità Strutturale, 41 (2017) 175-182.

Received: 28.02.2017
Accepted: 15.04.2017
Published: 01.07.2017

INTRODUCTION

A significant part of fracture mechanics deals with the determination of stress intensity factors and fracture toughness, used to predict the load as well as the angle of crack propagation. A large number of analyses has been carried out, and stress intensity factors at the crack tips are available in literature, for instance in the compendium by Murakami [1]. A case of interest in practical applications is that of a short crack emanating from a re-entrant corner in a body under general loading conditions, where often multiple-parameter characterization of the crack/notch tip stress/strain field is required. If the crack is short compared to the other sizes of the body, the effect of other free boundaries can be neglected and the loading experienced by the crack in this geometry is well described by the Williams asymptotic solution [2]. In particular, the problem of a smooth and frictionless crack lying on the projection line of a

three-quarter-infinite plane (Fig. 1) has been solved by Churchmann and Hills [3], by applying a distribution of dislocations along the line to clear the stresses coming from the Williams asymptotic fields.
Observing the cracks in many materials of common use, such as concrete, ceramic or rocks, it can be noted that the crack surfaces are not smooth but typically present a certain degree of tortuosity [4,5]. In this case, the assumption of smooth surfaces, which is commonly made in fracture mechanics, is acceptable only when a pure Mode I loading occurs, while the effects of roughness and friction cannot be neglected for Mode II or mixed mode loadings [6], since the normal and tangential displacements of a point along the crack are always coupled. We can note that this is precisely the case of the crack lying on the projection line of a three-quarter plane, because the asymptotic stress fields are uncoupled along the bisector of the re-entrant corner but we always have mixed mode loading on the projection line.
A simple way to take into account the effects of friction and roughness is to assume the crack surfaces as globally smooth and introduce the normal-tangential coupling along the contact surfaces, the so called *dilatancy*, through a rigid-plastic constitutive law [7], described by a slip rule and a slip potential. The presence of friction and roughness gives rise to a stress state on the crack surfaces which is dependent on the relative displacements between opposing points of the crack, thus the resulting problem is non-linear. The behaviour of smooth frictional cracks under cyclic loading has been for instance investigated in [8], with particular focus on the conditions of adaptation whereas shakedown analysis for discrete systems involving both friction and plasticity has more recently been studied in a very general form in [9].
In this paper, the effect of roughness and friction is taken into account for a crack emanating from a three-quarter-infinite plane (Fig. 1) and the resulting non-linear problem is solved using the iterative algorithm introduced in [6]. Stress intensity factors are computed for different values of the coefficient of friction and the roughness angle.

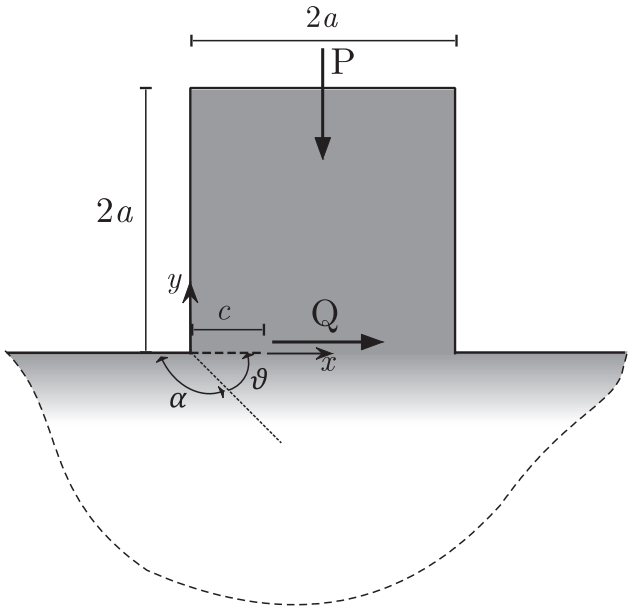

Figure 1: Sketch of the considered problem. A short crack c ≪ *a* is present along the projection line of a three quarter plane. Resultants of applied external loads are also shown.

FORMULATION

Crack problem solution

The Williams asymptotic solution is described by two eigenvalues λ_I, λ_{II} (which define the singularities of Mode I and Mode II stress fields, respectively), and the distribution of stresses resulting from the two eigenfunctions evaluated along the crack line:

$$\tau^{\infty}(x) = K_I^0 g_{r\theta}^I x^{\lambda_I - 1} + K_{II}^0 g_{r\theta}^{II} x^{\lambda_{II} - 1}$$
$$\sigma^{\infty}(x) = K_I^0 x^{\lambda_I - 1} + K_{II}^0 x^{\lambda_{II} - 1} \quad (1)$$

For the considered geometry, the internal wedge angle is $2\alpha = 3/2\pi$ and the angle corresponding to the line of the crack is $\vartheta = \pi/4$. Therefore we have:

$$\begin{aligned} &\lambda_I = 0.5445\ ,\ \lambda_{II} = 0.9085 \\ &g_{r\theta}^{I} = 0.543\ ,\ g_{r\theta}^{II} = -0.219 \\ &K_I^0 = 0.7304 K_I\ ,\ K_{II}^0 = -1.087 K_{II} \end{aligned} \tag{2}$$

where K_I^0, K_{II}^0 are simply scaled versions of the Mode I and Mode II notch stress intensity factors K_I, K_{II}, obtained from a calibration with the finite element method.

Let us consider the crack to be of length $c \ll a$ and lying along the x-axis. A distribution of edge dislocations of densities B_x, B_y is added, so that the resulting integral equations which govern the problem are the following:

$$\int_0^c B_x(\xi)\left[F_{xxy}(x,\xi) + \frac{1}{x-\xi}\right]d\xi + \int_0^c B_y(\xi) F_{yxy}(x,\xi)\,d\xi = -\frac{\pi(\kappa+1)}{2G}\left[\tau^{\infty}(x) + \sigma_t(x)\right] \tag{3}$$

$$\int_0^c B_x(\xi) F_{xyy}(x,\xi)\,d\xi + \int_0^c B_y(\xi)\left[F_{yyy}(x,\xi) + \frac{1}{x-\xi}\right]d\xi = -\frac{\pi(\kappa+1)}{2G}\left[\sigma^{\infty}(x) + \sigma_n(x)\right] \tag{4}$$

where G is the shear modulus, $\kappa = 3 - 4\nu$ is the Kolosov constant for plane strain, and ν is the Poisson ratio. The influence function $F_{kij}(x,\xi)$, connecting the stress component $\sigma_{ij}(x)$ to a dislocation $b_k(\xi)$, can be found in [3]. The right-side terms of Eqs. (3)-(4) contain the far-field stresses $\tau^{\infty}(x)$ and $\sigma^{\infty}(x)$, obtained from the Williams solution, and the shear and normal stresses applied to the crack surfaces, $\sigma_t(x)$ and $\sigma_n(x)$, respectively. Introducing the normalized variables t,s , with crack extremes $\pm$ 1, instead of x and ξ respectively, we can write the singular integral equations in the usual form, and express the unknown dislocation densities B_x, B_y as follows:

$$B_j(s) = \phi_j(s)\omega(s) = \phi_j(s)\sqrt{\frac{1+s}{1-s}}, \quad j = x, y \tag{5}$$

where we have chosen the fundamental form of the solution $\omega(s)$ to be singular at the crack tip $s = 1$ and bounded at $s = -1$. A numerical solution of the integral equations is needed, and this can be achieved by means of the Gauss-Chebyshev quadrature described in [10]. The resulting $2N$ equations in the $2N$ unknown $\phi_j(s_i)$ are the following:

$$\sum_{i=1}^{N} W(s_i)\left\{\phi_x(s_i)\left[F_{xxy}(t_k,s_i) + \frac{1}{t_k - s_i}\right] + \phi_y(s_i) F_{yxy}(t_k,s_i)\right\} = -\frac{\pi(\kappa+1)}{2G}\left\{\tau^{\infty}(t_k) + \sigma_t(t_k)\right\} \tag{6}$$

$$\sum_{i=1}^{N} W(s_i)\left\{\phi_x(s_i) F_{xyy}(t_k,s_i) + \phi_y(s_i)\left[F_{yyy}(t_k,s_i) + \frac{1}{t_k - s_i}\right]\right\} = -\frac{\pi(\kappa+1)}{2G}\left\{\sigma^{\infty}(t_k) + \sigma_n(t_k)\right\} \tag{7}$$

where $W(i)$ are the weight functions, s_i are the integration points at which the unknown functions and the displacements are computed, whereas t_k are the collocation points at which we evaluate the stresses. Stress intensity factors at the crack tip are directly related to the value of $\phi_j(s)$ for $s = +1$:

$$K_i = \frac{2G}{\pi(\kappa+1)}\sqrt{2\pi c}\,\phi_j(1), \qquad i = I, II, \quad j = x, y \tag{8}$$

Values of ϕ_j at end-points are not included in this quadrature method, thus Krenk's interpolation is used [11].

Interface constitutive law

In Eqs. (6)-(7), the stresses on the crack surface σ_t and σ_n are related to the relative displacements by means of a constitutive law which describes friction and roughness. According to this law, the crack surfaces are assumed to be

globally smooth, with the effect of friction and roughness built in a rigid-plastic constitutive relationship. Let us consider the relative tangential and normal displacements between two points situated on opposite positions on the crack surfaces, Fig. 2(a):

$$\begin{aligned} w_t &= u_x^{+} - u_x^{-} \\ w_n &= u_y^{+} - u_y^{-} \end{aligned} \tag{9}$$

where superscripts + and - indicate the superior and inferior surface of the crack, respectively. Tangential and normal relative displacement increments are additively composed of a recoverable elastic part dw_i^e and a non-recoverable plastic part dw_i^p:

$$dw_i = dw_i^e + dw_i^p, \qquad i = t, n \tag{10}$$

where subscript i is used to denote the vector components t and n. The stress that the interface supports is assumed to be related to the elastic part by the following expression:

$$d\sigma_i = E_{ij} dw_j^e \tag{11}$$

where E_{ij} is the interface stiffness (summation convention is applied to repeated indices). Here, we assume $E_{ij} = 0$ for $i \neq j$ and assure that they are relatively large compared to the stiffness of the adjacent medium, by applying a penalty two to four orders of magnitude greater to the shear modulus G of the medium itself. The permanent part of the deformation is given by the following slip rule:

$$dw_i^p = \begin{cases} 0 \;\; if \;\; F < 0 \;\; or \;\; dF < 0 \\ \lambda \dfrac{\partial G}{\partial \sigma_i} \;\; if \;\; F = dF = 0 \end{cases} \tag{12}$$

where F is the slip function and G is the slip potential. It can be noted that, since the friction law is non associated, F and G do not coincide, and the direction of slip is given by the gradient of G. Combining (10)-(12), we obtain the fundamental relationship which connects the stresses along the crack to the relative displacements:

$$d\sigma_i = E_{ij}^{EP} dw_j \tag{13}$$

where:

$$\begin{aligned} E_{ij}^{EP} &= E_{ij} \;\; \text{if } F < 0 \text{ or } dF < 0 \\ E_{ij}^{EP} &= E_{ij} - \frac{\dfrac{\partial F}{\partial \sigma_p} E_{iq} E_{pj} \dfrac{\partial G}{\partial \sigma_q}}{\dfrac{\partial F}{\partial \sigma_p} E_{pq} \dfrac{\partial G}{\partial \sigma_q}} \;\; \text{if } F = dF = 0 \end{aligned} \tag{14}$$

We chose to describe the roughness by means of a saw-tooth model, with identically shaped asperity surfaces whose size is characteristic of the type of discontinuity being modelled, Fig. 2(b). Moreover, we assume that the amount of tangential sliding is small enough so that the asperity peak of one surface does not override that of the other surface. The slip function and slip potential are the following:

$$\begin{aligned} F &= \left| \sigma_n \sin\alpha_k + \sigma_t \cos\alpha_k \right| + \mu(\sigma_n \cos\alpha_k - \sigma_t \sin\alpha_k) \\ G &= \left| \sigma_n \sin\alpha_k + \sigma_t \cos\alpha_k \right| \end{aligned} \tag{15}$$

where α_k represents the angle of the active k asperity surface and μ is the coefficient of friction of the Coulomb law. If roughness is not taken into account, only friction is present and, therefore, Eqs. (15) become simpler:

$$F = |\sigma_t| + \mu\sigma_n$$
$$G = |\sigma_t| \tag{16}$$

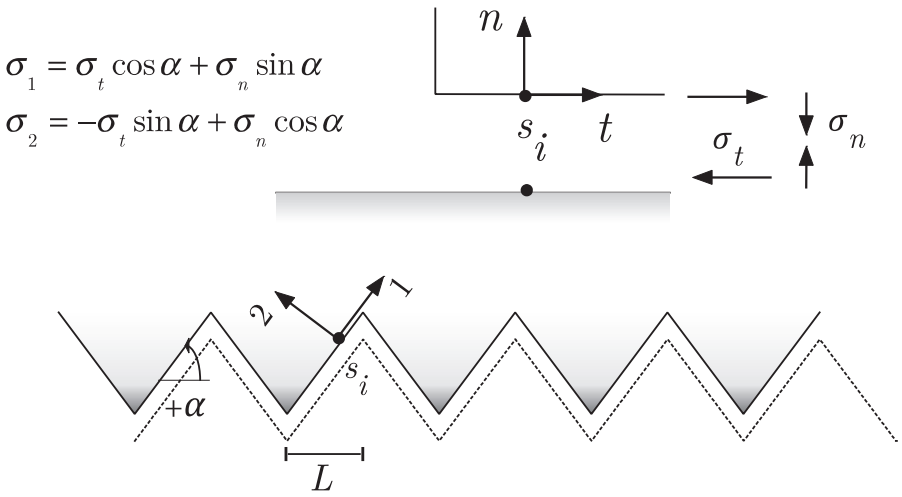

Figure 2: Schematic representation of the model used to describe the roughness of the crack surfaces. (a) Local tangent-normal coordinate system at a contact point pair (shown separately for clarity). (b) Saw-tooth asperity model, with constant angle and asperity length. Relationships for stresses between the two coordinate systems are also shown.

Compliance matrix

To efficiently solve the problem, a compliance matrix $\boldsymbol{C}$ that relates the stresses, arising at the collocation points from the applied loads, to the values of the relative displacements of the crack at the integration points can be obtained. The details of this procedure are presented in [6]. Displacements along the crack, in an incremental form, are related to stresses by the following expression:

$$[d\mathbf{w}_t, d\mathbf{w}_n]^T = \mathbf{C}[d\tau^\infty + d\sigma_t, d\sigma^\infty + d\sigma_n]^T \tag{17}$$

where we have collected the increments of stresses and displacements in ordered vectors, such that, for instance, we have $d\boldsymbol{w}_t = [dw_{1t}, \ldots dw_{Nt}]^T$, with subscripts $i = 1,\ldots,N$ referring to the integration points along the crack. Now the problem in (6)-(7) takes the following formulation:

$$(\mathbf{I} - \mathbf{C}\mathbf{E}^{EP}\mathbf{T})[d\mathbf{w}_t, d\mathbf{w}_n]^T = \mathbf{C}[d\tau^\infty, d\sigma^\infty]^T \tag{18}$$

where $\boldsymbol{I}$ is the identity matrix and $\boldsymbol{E}^{EP}$ is the matrix containing the terms described in Eq. (14). We have introduced a transformation matrix $\boldsymbol{T}$ to express crack displacements at the collocation points in terms of those at the integration points, so that the constitutive law in (13) can be enforced. This matrix is built using Krenk's interpolation formula [11], in order to obtain the values of the unknown functions in points along the crack which are different from the integration points.

Eq. (18) is a system of non-linear algebraic equations in the $2N$ unknown incremental relative displacements, to be solved by taking small increments in far-field loading. The stiffness matrix $\boldsymbol{E}^{EP}$ needs to be updated at each step, using the displacement-stress configuration from the previous step. By using the compliance matrix, the dislocation densities at each step are not needed to be integrated in order to compute the relative displacements along the crack and, therefore, the efficiency of the algorithm is increased.

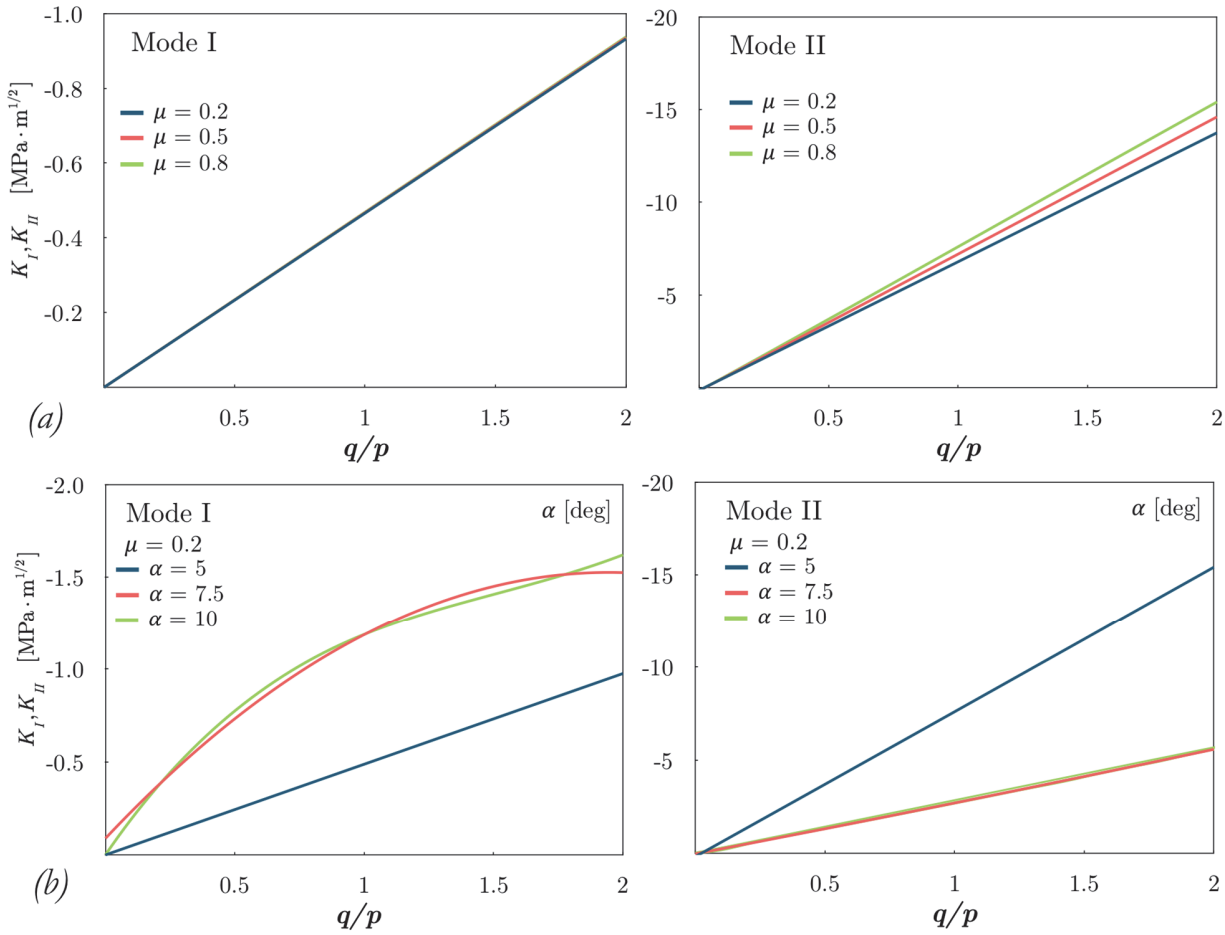

Figure 3: Stress intensity factors as functions of the applied stresses. (a) The case of smooth surfaces, with different values of the coefficient of friction μ. (b) The effect of roughness is included and trends are shown for different values of the asperity angle α.

RESULTS

We now present the results we have obtained for the example problem in Fig. 1, consisting of an elastic punch welded to a half-space made of the same material. The elastic modulus is E = 30GPa and the Poisson coefficient is ν = 0.25; the fracture toughness of the material is K_{Ic} = 1.1 MPa$\sqrt{m}$. A state of plane strain is assumed. A crack of length $c = 0.2a$ is present, whose surface model is described by the coefficient of friction μ and the constant roughness angle α_k. The external loading applied consists of a constant pressure p = P/$2a$ and a shear traction q= Q/$2a$ which is monotonically increased in time.

Fig. 3 displays the plots of the stress intensity factors as functions of the far-field shear stress. Fig. 3(a) is related to the case of smooth surfaces (α=0), where only friction is present. We can note that the effect of friction is rather modest, anyway a slight increment of the absolute value of Mode II factor with increasing friction is observed. Fig. 3(b) plots the stress intensity factors for different values of the asperity angle α. The trends show that, as the angle α increases, the absolute value of Mode I stress intensity factor K_I increases, while the absolute value of K_{II} decreases (note that they are both negative). This behaviour can be explained considering the effect of dilatancy, which affects K_I, and the effect of roughness, which increases the resistance to sliding displacements, therefore reducing the absolute value of K_{II}. However, one should be careful to generalize this behaviour, which can be completely different as the coefficient of friction also increases. In this sense, more research is needed to further investigate the issue.

Fig. 4 displays the dimensionless fracture propagation stress q_{max}/p as a function of the coefficient of friction, in the case of smooth surfaces. Here, the classical mixed-mode criterion of maximum tangential stress is considered [12] and the

fracture propagation stress is obtained when the combined factor K_{eff} equals the fracture toughness K_{Ic} of the material. According to the fracture criterion we have:

$$K_{eff} = K_I \cos^3(\theta/2) - 3K_{II} \cos^2(\theta/2)\sin(\theta/2) \tag{19}$$

where ϑ is the angle at which the crack will extend, obtained from the following expression:

$$\tan(\theta/2) = 0.25K_{II} / K_I \pm 0.25(K_{II}^2 / K_I^2 + 8)^{1/2} \tag{20}$$

The effect of friction on fracture initiation is notable in Fig. 4: a strong increment in the fracture propagation stress is observed, whereas the propagation angle ϑ slightly decreases (note that the maximum value for pure Mode II would be 70.5° [13]).

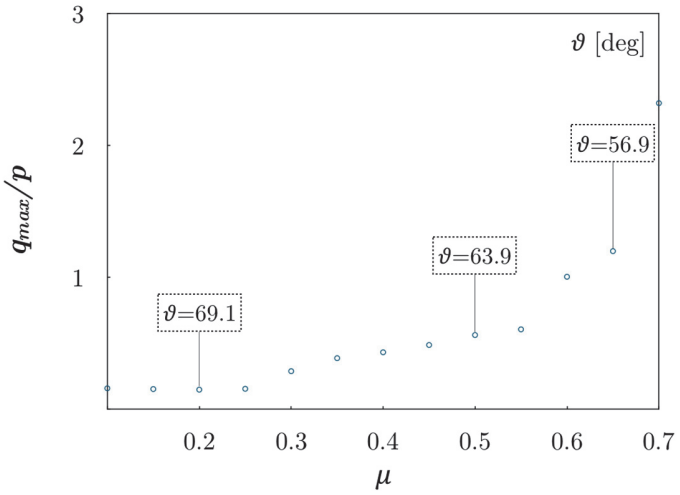

Figure 4: Smooth surfaces (α=0). Fracture propagation stress q_{max} is shown for different values of the coefficient of friction μ. The corresponding propagation angle ϑ is also shown.

CONCLUSIONS

In this study, we describe the mixed-mode tip stress field of a crack emanating from a re-entrant corner, using the Williams solution in combination with an appropriate edge dislocation distribution along the crack line. The behaviour of a rough and frictional crack is conveniently described by an interface model where a rigid-plastic constitutive relationship between stresses and relative displacements along the crack and a slip function with non-associated flow are used. The results we have obtained clearly show that the effect of friction and roughness is remarkable. In particular, the effect of dilatancy increases the values of the (negative) Mode I stress intensity factor while it simultaneously reduces the Mode II factor when the roughness angle increases. Moreover, the fracture propagation load is strongly influenced by friction.

REFERENCES

[1] Murakami, Y. (Ed.), Stress Intensity Factors Handbook, vol. 1, Pergamon Press, New York, (1987).
[2] Williams, M.L., Stress singularities resulting from various boundary conditions in angular corners of plates in extension, J. Appl. Mech., 19 (1952) 526–528.
[3] Churchman, C.M., Hills, D.A., The edge dislocation in a three-quarter plane. Part II: Application to an edge crack, Eur. J. Mech. A Solids, 25 (2006) 389–396.

[4] Carpinteri, An., Spagnoli, A., Vantadori, S., Viappiani, D., Influence of the crack morphology on the fatigue crack growth rate: a continuously-kinked crack model based on fractals, Eng. Fract. Mech., 75 (2012) 579-589.
[5] Brighenti, R., Carpinteri, An., Spagnoli, A., Scorza, D., Crack path dependence on inhomogeneities of material microstructure, Frattura ed Integrità Strutturale, 20 (2012) 6-16.
[6] Ballarini, R., Plesha, M.E., The effects of crack surface friction and roughness on crack tip stress fields, Int. J. Fract., 34 (1987) 195–207.
[7] Plesha, M.E., Constitutive models for rock discontinuities with dilatancy and surface degradation, Int. J. Numer. Anal. Methods Geomech., 11 (1987) 345–362.
[8] Carpinteri, Al., Scavia, C., Energy dissipation due to frictional shake-down on a closed crack subjected to shear, Meccanica, 28 (1993) 347-352.
[9] Klarbring, A., Barber, J.R., Spagnoli, A., Terzano, M., Shakedown of discrete systems involving plasticity and friction, Eur. J. Mech. A Solids, 64 (2017) 160-164.
[10] Erdogan, F., Gupta, G.D., Cook, T.S., Numerical Solution of Singular Integral Equations, in: Sih, G.C. (Ed.), Methods of Analysis and Solutions of Crack Problems, Noordhoff, Groningen, (1973) 368–425.
[11] Hills, D.A., Kelly, P.A., Dai, D.N., Korsunsky, A.M., Solution of Crack Problems – The Distributed Dislocation Technique, Kluwer Academic, Dordrecht, (1996).
[12] Sih, G. C., Strain-energy-density factor applied to mixed mode crack problems, Int. J. Fract., 10 (1974), 305-321.
[13] Erdogan, F., Sih, G.C., On the crack extension in plates under plane loading and transverse shear, J. Basic Eng., 85 (1963) 519–527.